SHEAR FAILURE CRITERION FOR RC T-BEAMS

Gregoria M. Kotsovou, Demitrios M. Cotsovos

Heriot-Watt University, Edinburgh, UK

Abstract

The paper is concerned with the development of a failure criterion capable of accurately predicting the shear capacity of reinforced concrete T-beams while correctly accounting for the beneficial effect of the increase of the compressive zone due to the presence of flanges. The development of the subject criterion is based on an alternative design method (the compressive force path method) that leads to predictions of reinforced concrete structural behaviour and design solutions considerably different compared to those of the current design codes without however compromising structural performance requirements (mainly associated with ductility and strength). The validity of the proposed failure criterion is verified through a comparative study of the calculated values with their experimentally-established counterparts obtained from an extensive literature survey. Through this comparative study it is demonstrated that the predictions of the proposed criterion provide a closer fit to the available experimental data than their counterparts obtained from the design codes considered.

Keywords: compressive force path theory; design; failure criteria; reinforced concrete; T-beams

List of notations

a_v shear span

b, b_w width of beams web

d effective depth

h_f flange height

Ï ratio of tensile longitudinal reinforcement

f_t strength of concrete in direct tension

f_{yv} yield stress of transverse reinforcement

A_{sv} cross sectional area of transverse reinforcement within a length of 2*d* extending symmetrically on either side of the location of 2.5*d* from the closest beam support.

ΔM bendingmoment increment

ΔT bond force

V shear force

$T_{II,1}$ maximum transverse tensile force sustained by concrete in the compressive zone at a distance of 2.5*d* from nearest support for beams with a rectangular cross section and $a_v/d > 2.5$.

$T_{II,1f}$ portion of $T_{II,1T}$ (see below) developing in flange

$T_{II,1T}$ $T_{II,1}$for a T-beam with $a_v/d > 2.5$.

$V_{II,1}$ maximum shear force sustained at cross section at a distance of 2.5*d*from nearest support for beams with a rectangular cross section and $a_v/d > 2.5$.

$V_{II,1,T}$ $V_{II,1}$for a T-beam with $a_v/d > 2.5$.

INTRODUCTION

Experimental information, which is used in the work presented herein, shows that reinforced concrete (RC) beams with a T-shaped cross section exhibit values of shear capacity which are higher, often by a significant amount, than those characterising RC beams with a rectangular cross section [1]. Such behaviour can be attributed to the increase of the beams' compressive zone due to the presence of the flange, the effect of which on shear capacity is not allowed for in current design practice. This is because, in accordance with the simplified beam theory which underlies shear design methods, any increase in shear capacity due to the increase of the width of the compressive zone is, to a large extent, counteracted by the decrease of the shear stresses within the flange as they spread along the flange width (see Fig. 1).

Therefore, there is an inherent difficulty in allowing for the flange's effect on shear capacity without a modification of the concepts underlying shear design methods. And yet, allowing for this effect may lead to a reduction of the amount of transverse reinforcement required to safeguard against shear failure. This may be true, not only when concrete in the presence of transverse reinforcement is considered to contribute to shear capacity (ACI 318 2014 [2]), but also when the concrete's contribution is ignored (EC2 2004 [3]). In the latter case, if the flange's effect on shear capacity were allowed for, the code criterion for specifying reinforcement may not be fulfilled and, therefore, a nominal amount of transverse reinforcement may be sufficient.

In view of the above, the aim of the present work is the development of a failure criterion which allows for the effect of the compressive zone's size on shear capacity. The work will be based on concepts which underlie the Compressive Force Path (CFP) theory [4], since this is the only theory proposed to date which links the causes of an RC beam's failure to the stress conditions in the compressive, rather than the tensile zone. The validity of the proposed criterion will be verified through a comparison of its predictions with experimental data obtained from the literature. The comparison will also include the values predicted by current codes (ACI 318 2014 [2], EC2 2004 [3]), as well as an empirical formula, which has been developed so as to allow for the effect of the compressive zone's shape and size on shear capacity and included in the guidance for "design and detailing of concrete structures for fire resistance" of The Institution of Structural Engineers, London 1978 [5].

BACKGROUND

Shear resistance and force transfer

In accordance with the CFP theory [4], the shear resistance of the tensile zone of RC beams becomes negligible, if any, after the formation of flexural and/or inclined cracks. This is because cracking diminishes the shear stiffness of concrete and causes stress redistribution towards the stiff crack-free concrete of the compressive zone; thus, the latter becomes the sole contributor to the beam's shear resistance. Moreover, it has been demonstrated [4] that such behaviour is compatible with the experimentally-established behaviour of concrete as a material as regards both its stress-strain behaviour and its cracking mechanism, the latter involving crack extension in the direction of cracking and opening in the orthogonal direction, thus precluding any shear movement of the crack faces that may be resisted by aggregate interlock and dowel action as widely assumed.

In view of the above, internal force transfer is accomplished by the compressive zone through a beam-like action mechanism schematically described in Fig. 2. From the figure, it can be seen that, under the action of the bond force,ΔT, developing at the interface between concrete and flexural steel, concrete cantilevers (such as that indicated in Fig. 2(a)) which form between successive flexural or inclined cracks, subject the compressive zone to a momentΔM (see Fig. 2(b)) which transfers the shear force V acting on the right-hand side of the portion to which the cantilever is fixed to the left-hand side (see Fig. 2(c)).Moreover, it has been shown that the presence of triaxial compressive-stress conditions developing for purposes of transverse deformation compatibility enables the compressive zone to sustain alone the total action of V [4], commonly assumed to be sustained by the beam cross section.

Shear failure and underlying causes

In accordance with the experimental findings of Kani (1964) [6], RC beams, without transverse reinforcement, with shear span-to depth ratios (a_v/d) ranging between 1 and a value (dependent on the reinforcement ratio ρ) of the order of 5, exhibit load carrying capacities smaller than that corresponding to flexural capacity (see Fig. 3). The causes of such 'premature' loss of load-carrying capacity are attributed by the CFP theory to longitudinal spitting of the compressive zone which may occur when the transverse component of the compressive stress field referred to at the bottom of the preceding section becomes tensile [4]. Therefore, transverse reinforcement may be required for preventing such splitting, rather than for improving the shear capacity of the beam's cross section as widely considered.

More specifically, for $1 < a_v/d \leq 2.5$, the deep inclined crack which forms within the shear span penetrates deeply into the compressive zone causing a type of failure which is commonly referred to as shear-compression failure [7]. However, it has been shown that this is essentially a flexural type of failure which is brittle in nature in that concrete in the compressive zone fails before yielding of the flexural reinforcement [4]. A similar type of failure may be suffered by RC beams with $a_v/d >$ 2.5 in the region of load points where the large bending moment combines with a large shear force. This is one of the two types of failure characterising beams with $a_v/d >$ 2.5 commonly referred to as diagonal-tension failures [7]; it takes the form of longitudinal splitting of the compressive zone which gives the impression that it forms extension of a major inclined crack the formation of which invariably precedes failure of this type of beams [4]. However, the most usual type of failure suffered by such beams is horizontal splitting of the compressive zone occurring at a distance of around 2.5*d* from the nearest support [4]. As shown in Fig. 4, such splitting occurs independently of any other form of cracking in the region of the compressive zone between the tip of the deepest inclined crack and the extreme compressive fibre of the beam; it is referred to as type II failure at location 1 (location at a distance of 2.5*d* from nearest support), in short type II,1 failure [4].

Proposed flange contribution to 'shear' capacity

For the flexural types of failure referred to in the preceding section (which are premature in that failure of the compressive zone occurs before yielding of the flexural reinforcement), the effect of the presence of the flange on flexural capacity is allowed for by any of the methods developed to date for calculating flexural capacity. In contrast with these methods, the presence of the flange is ignored when calculating the tensile force $T_{II,1}$ which, in accordance with the CFP theory is sustained by concrete in the region of the tip of the deep inclined crack just before horizontal splitting of the compressive zone. As discussed in what follows, $T_{II,1}$ is obtained from [4]

$$T_{II,1} = 0.5 f_t b d \quad (1)$$

Where$b$ and d are the width and effective depth of the web and f_t the strength of concrete in direct tension.

$T_{II,1}$ (which is numerically equal to the shear force $V_{II,1}$at the cross section at a distance of 2.5d from the nearest support [4]) is essentially the resultant of the tensile stresses which develop for local equilibrium purposes in the region of the compressive zone where the horizontal flow of the compressive stresses developing on account of bending takes an inclined direction towards the support (see Fig. 5). By invoking the Saint Vennant's principle, the rapidly diminishing tensile stresses with a peak value of f_t at a distance of 2.5d from the nearest support have been replaced with a uniform stress distribution with intensity 0.25f_t extending to a distance of d on either side of the location of the peak stress value f_t throughout the cross section's width b (see Fig. 6). Equation (1) expresses the product of the uniform stress 0.25f_t

with the area b ($2d$) over which the uniform stress develops, i.e. $T_{II,1}$ = (0.25 f_t) b ($2d$) = 0.5 $f_t b\ d$.

For T-beams, equation (1) may be modified so as to allow for the presence of the flange by following a similar reasoning. By invoking Saint Vennant's principle, the tensile stresses developing in the compressive zone due to change in the direction of the flow of the compressive stresses will be assumed to diminish in the manner indicated in Fig. 6not only in the longitudinal, but also in the transverse direction across the cross-section's width within the flange to a distance of h_f on either side of the web, where h_f is the depth of the flange at its intersection with the web. By adopting a uniformly distributed tensile stress of $0.25f_t$ in the longitudinal direction underlying the derivation of equation (1), the 'true' distribution of the tensile stresses in the flange is replaced with a unifirm stress distribution with intensity 0.25 (0.25 f_t), where 0.25 f_t is (in accordance with equation (1)) the intensity of the uniform stress distribution in the web (see Fig. 7). Then, the additional tensile force sustained by the flange over a length $2d$ (where d is the effective depth of the beam) will be:

$$T_{II,1,f} = 2(0.25)(0.25f_t)h_f(2d) = 0.5^2 f_t h_f d. \quad (2)$$

Therefore, the total force sustained by the T-beam becomes

$$T_{II,1,T} = 0.5f_t b_w d + 0.5^2 f_t h_f d = 0.5f_t(b_w + 0.5h_f)d \quad (3)$$

with $T_{II,1T}$ being numerically equal to the shear force $V_{II,1T}$ developing at the same location.

VERIFICATION

Information used

The verification of the ability of equation (3) to produce realistic predictions of the shear force corresponding to failure at the location of T-beams (without transverse reinforcement) at a distance of 2.5*d* from the nearest support has been based on comparing the equation's predictions with the values of shear capacity established from tests on T-beams reported in the literature. The effect of the presence of transverse reinforcement is also discussed by reference to experimental information on T-beams with transverse reinforcement. The design details of the test specimens without and with transverse reinforcement are shown in Tables 1 and 2, respectively, which also provides the experimentally-established values of shear capacity.

For the beams without transverse reinforcement, the values of shear capacity predicted by the proposed formula are shown in Table 3. For comparison purposes, the table also includes the values predicted by the formulae adopted not only by ACI 318 (2014) [2] and EC2 (2004) [3], which do not allow for the contribution of flanges on shear capacity, but also by the formula proposed by the Institution of Structural Engineers, London (1978) [5], which allows for the contribution of the flange. The latter formula is given in Appendix. In order to establish whether the above formulae are capable of predicting the mode of failure of the specimens investigated, the values of shear corresponding to flexural capacity are also included in the table. For the case of the proposed formula, flexural capacity was assessed in accordance with the CFP theory, since the proposed formula was derived within the context of this theory, whereas in all other cases the values of flexural capacity resulted from the relevant code-adopted methods. The predicted values of shear capacity expressed in a normalized form (i.e. the ratios of the predicted values to their experimentally-established counterparts) are included in Table 4 and presented in the form of Gaussian distributions in Fig. 8. The evaluation of the validity of the formulae used to calculate shear capacity is essentially based on the use of these normalized values.

The effect of the presence of transverse reinforcement is established by reference to the information provided in Tables 5 and 6. The tables include information for T-beams with shear reinforcement similar to that provided in Tables 3 and 4 for T-beams without such reinforcement. It should be noted, however, that in Table 5 the calculated values of shear capacity resulting from the proposed formula are marked with 'c' when they are larger than the values expressing the tensile force sustained by the transverse reinforcement within the length where transverse tension $T_{II,1}$ develops. When the opposite is the case, the values of shear capacity are those expressing the tensile force sustained by the transverse reinforcement at yield and marked with 's' in the table. As for the case of the results in Table 4, the normalised values of 'shear' capacity included in Table 6 are also presented in the form of Gaussian distributions in Fig. 9

Beams without reinforcement

From Table 3, it can be seen that, with the exception of the values V_f and V_c of shear corresponding to flexural and shear, respectively, capacities resulting from the application of the IStrcutE guidance, the condition V_f>V_c is fulfilled for all values obtained from the other methods of calculation. This is indicative of a shear mode of failure which is in agreement with the experimental results. As regards the values obtained from the application of the IStructE methods, in 26 out of the 30 cases investigated V_f>V_c is also fulfilled. However, for the 4 remaining cases V_f is only slightly smaller than V_c with the difference between the two values being well within the scatter of the predicted values of shear capacity indicated by the standard deviation included in Table 4.

From Fig. 8 and Table 4, it can be seen that the values obtained from the proposed formula correlate very closely with the experimental findings. The deviation of the predicted values from their experimentally-obtained counterparts is on average only 3%. In contrast with the proposed formula, those adopted by ACI 318 and EC2 underestimate shear capacity by over 30%. As discussed in the introduction, such an underestimation is expected, since the concepts underlying the derivation of the code formulae do not allow for the effect of the beam's flange on shear capacity. On the other hand, the formula proposed by IStructE, which allows for the effect of the flange, is found to overestimate shear capacity by an amount over 30% on average. The cause for this overestimation may be attributed to the data used for the calibration of this formula. These data were primarily obtained from tests on beams with transverse reinforcement designed so as to prevent shear failure.

Beams with transverse reinforcement

It should be reminded at this stage that in accordance with ACI 318 and IStructE both concrete and transverse reinforcement contribute to a beam's shear capacity. The contribution of concrete V_c is obtained from the formulae used to calculate the shear capacity of beams without transverse reinforcement, whereas that of the transverse reinforcement is equivalent to the tensile force V_s sustained by the stirrups at yield contributing to the formation of the transverse tie at the most critical location of the truss model which underlies the shear design method. On the other hand, in accordance with EC2 and the CFP theory (within the context of the latter the proposed formula has been derived), shear capacity is provided either by concrete only when $V_c > V_s$, or transverse reinforcement only when $V_c<V_s$, with V_c being calculated as for the case of beams without transverse reinforcement. For the case of EC2, V_s is calculated on the basis of the reasoning underlying the methods in accordance with ACI 318 and IStructE, whereas in accordance with the CFP theory is equal to the tensile force sustained by the transverse reinforcement (A_{sv}) within a length of 2d extending symmetrically on either side of the location at a distance of 2.5d from the closest beam support, i.e.

$$V_s = A_{sv} f_{yv} \tag{4}$$

where f_{yv} is the yield stress of the reinforcement.

It is also important to note that the development of all methods has been intended to safeguard a flexural mode of failure; and yet, their validity appears to have been tested against experimental information obtained from tests on beams in which the specified amount of reinforcement is insufficient to fulfill this aim. In fact,

Table 5 shows that in all but two cases the tested beams failed in shear. From the table, it is found that, as for the case of the T-beams without transverse reinforcement, with the exception of the IStructE methods, all other methods are capable of predicting correctly the mode of failure of the beams. The IStructE method incorrectly predicted a flexural, rather than a shear, mode of failure in 4 out of the 57 cases investigated. However, as for the case of the beams without transverse reinforcement (see Table 3), V_f in these 4 cases is smaller than V_c by an amount well within the scatter of the calculated values of shear capacity indicated in Table 6 in the form of standard deviation.

Since, as indicated in Table 5, nearly all specimens tested exhibited a shear mode of failure, it is not possible to establish, on the basis of the information provided in Table 6, which of the design methods considered herein is capable of achieving the aims of structural design in the most efficient manner, i.e., the smaller possible amount of transverse reinforcement. What becomes clear from Table 6 and Fig. 9, however, is that, with the exception of IStructE, in all other cases shear capacity is underestimated by an amount which, on average, ranges between 30% and 40%. Moreover, even for IStructE, which overestimates shear capacity by less than 3%, this overestimate is considerably smaller than the nearly 40% overestimate exhibited for the beams without transverse reinforcement (see Table 4).

It appears from the above, therefore, that the provision of transverse reinforcement increases shear capacity. Such an increase is considered to reflect the effect of transverse reinforcement on the cracking processes of concrete. It is well known that a crack forms and extends in the direction of the maximum principal compressive stress and, concurrently, opens in the orthogonal direction [9]. As discussed earlier, in accordance with the CFP theory, the type of shear failure investigated herein is caused by horizontal splitting of the compressive zone at a location situated at a distance of 2.5*d* from the nearest support. Since the horizontal direction is the direction of the maximum principal compressive stress, crack extension occurs concurrently with crack opening in the orthogonal (i.e., transverse) direction. The presence of transverse reinforcement reduces the rate of crack opening and, hence, the rate of crack extension, thus leading to an increase of shear capacity, since a higher load is required for crack extension to continue to failure of the beam.

CONCLUSIONS

The work described in the paper has been developed with the context of the CFP method. Within this context it has been possible:

- to identify the type of failure for which current failure criteria do not allow for the effect of the flanges on the load-carrying capacity of RC T-beams;
- to complement an existing simple failure criterion developed for RC beam/column elements with a rectangular cross section so as to extend its range of application to the case of RC T-beams;
- to verify the validity of the proposed failure criterion through a comparative study of the calculated values of shear capacity with their experimentally-established counterparts obtained from the literature after an extensive survey.
- to link the beneficial effect of the transverse reinforcement on load-carrying capacity to the restraining effect that the presence of such reinforcement has

on crack opening which delays the extension of the cracking processes to failure.

The implementation of the proposed failure criteria in practice is expected to lead to a reduction of the amount of transverse reinforcement required for safeguarding against shear failure. This is of particular importance in bridge girders with a T-shaped or box cross section in which there is a smooth transition from the web width to the flange.

Acknowledgments

This research was supported by the HORIZON 2020 Marie Skłodowska-Curie Research Fellowship Programme H2020-660545, titled: ANALYSIS OF RC STRUCTURES EMPLOYING NEURAL NETWORKS (ARCSENN).

REFERENCES

[1] Thamrin R., Tanjung J., Aryanti R.,Nur O.F. and Devinus A. Shear Strength of Reinforced Concrete T-Beams Without Stirrups. Journal of Engineering Science and Technology 2016; 11(4): 548-562.

[2] American Concrete InstituteBuilding Code Requirements for Structural Concrete (ACI 318M-14) and Commentary (ACI 318MR-14) 2014.

[3] British Standards, BS EN 1992-1-1: 2004. Eurocode2 (EC2): Design of concrete structures. Part 1-1: General rules and rules for buildings.

[4] Kotsovos M.D. Compressive Force-Path Method: Unified Ultimate Limit-State Design of Concrete Structures. Springer (London), 2014.

[5] The Institution of Structural Engineers. Design and detailing of concrete structures for fire resistance. Interim guidance by a Joint Committee of the Institution of Structural Engineers and The Concrete Society, 1978.

[6] Kani G. N.J. The Riddle of Shear and its Solution. Journal of the American Concrete Institute Proceedings 1964; 61(4): 441-467.

[7] Kong F. K. and Evans R. H. Reinforced and Prestressed Concrete. Van Nostrand Reinhold (UK), 1987.

[8] Kotsovos M.D. and Newman J.B. Fracture Mechanics and Concrete Behaviour. Magazine of Concrete Research1981; 33(115): 103-112.

[9] Bousselham A. and Chaallal O. Behavior of Reinforced Concrete T-Beams Strengthened in Shear with Carbon Fiber-Reinforced Polymer – An Experimental Study.ACI Structural Journal 2006; 103(3): 339-347.

[10] Ferguson P.M. and Thompson J.N. Diagonal Tension in T-Beams Without Stirrups. Journal of the American Concrete Institute 1953; 49(3): 665-675.

[11] Kotsovos M.D., Bobrowski J. and Eibl J. Behaviour of reinforced concrete T-beams in shear. The Structural Engineer 1987;65B(1): pp. 1-10.

[12] Panda K.C., Bhattacharyya S.K. and Bairai S.V. Strengthening of RC T-beams with Shear Deficiencies Using GFRP Strips. Journal of Civil Engineering and Architecture2011; 5(1): 56-67.

[13] Placas A. and Regan P.E. Shear Failure of Reinforced Concrete Beams. ACI Journal 1971;68(10): 763-773.

[14] Sahoo D.R., Bhagat S. and Reddy T.C.V. Experimental study on shear-span to effective-depth ratio of steel fiber reinforced concrete T-beams. Materials and Structures2015; 49: 3815-3830.

[15] Wehr K. E. Shear strength of reinforced concrete T-beams. Research report No. 4 on Joint research highway project, Purdue University Lafayette Indiana, USA, 1967.

[16] Koutas L. and Triantafillou T.C. Use of Anchors in Shear Strengthening of Reinforced Concrete T-Beams with FRP. Journal of composites for Construction 2013; 17(1): 101-107.

[17] Leonhardt F. and Walther R. Schubversuche an Einfeldringen Stahlbetonbalken mit und ohne Schubbewehrung zur Ermittlung der Schubtragfähigkeit und der Oberen Schubspannungsgrenze. Heft 151, Deutcher Ausschuss für Stahlbeton, W. Ernst & Sohn, Berlin, 1962; 68 pp. (in German)

[18] Leonhardt F. and Walther R. Schubversuchean Platten balken mit unterschiedlicher Schubbewehrung. Heft 156, Deutcher Ausschuss für Stahlbeton, W. Ernst & Sohn, Berlin, 1963, 84 pp. (In German)

[19] Sorensen H. C. Shear tests on 12 reinforced concrete T-beams. Structural Research Laboratory, Technical University of Denmark, Report No. 60, 1974.

[20] Spagnolo L.A., Sanchez Filho, E.S., and Velasco M.S. Libracon. Structures and Materials Journal,2013;6(1): 1-12.

APPENDIX :Calculation of shear strength according to current codes and IStructE methods

EC2

Shear capacity of concrete for members without axial loading and shear reinforcement is given byexpression (A.1)

$$V_{Rd,c} = \left[C_{Rd,c} k (100 \rho_l f_{ck})^{1/3}\right] b_w d \tag{A.1}$$

where,

$C_{Rd,c}$ is taken as 0.18/γ_c

$$k = 1 + \sqrt{\frac{200}{d}} \leq 2.0$$

$$\rho_l = \frac{A_{sl}}{b_w d}$$

A_{sl} is the area of the tensile reinforcement (mm^2)

b_w is the smallest width of the cross-section (mm)

d is the effective width (mm)

f_{ck} is the compressive concrete strength (MPa)

If the member has shear reinforcement then, according to the truss theory, all the shear resistance of the member is sustained by the yielding shear reinforcements according to expression(A.2)

$$V_{Rd,s} = \frac{A_{sw}}{s} z f_{ywd} cot\theta \tag{A.2}$$

where

A_{sw} is the cross-sectional area of the shear reinforcement (mm^2)

s is the spacing of the stirrups (mm)

z is the lever arm and approximately equal to 0.9d (mm)

f_{ywd} is the design yield strength of the shear reinforcement (MPa)

θ is the angle between concrete compression struts and the main tension chord

The value of θ is limited to $1 \leq cot\theta \leq 2.5$ and is obtained by setting $V_{Rd,s}$ equal to the maximum shear force,$V_{Rd,max}$, which can be sustained by the member limited by crushing of the compression struts as

$$cot\text{Î¸} = \sqrt{\frac{b_w v f_{cd}}{\frac{A_{sw}}{s} f_{ywd}} - 1} \quad \text{(A.3)}$$

where

$$v = 0.6\left[1 - \frac{f_{ck}}{250}\right]$$

ACI318

For a non prestressed member without axial load and shear reinforcement, shear is assumed to be resisted by the concrete,V_c, as

$$V_c = 0.17\text{Î»}\sqrt{f_c} b_w d \text{ (MPa)} \quad \text{(A.4)}$$

with Î» equal to 1 for vertical stirrups

For a non prestressed member without axial load, but with shear reinforcement, a portion of the shear strength is assumed to be provided by the concrete, V_c, and the remainder by the shear reinforcement, V_s, withthe shear resistance being calculated by the sum of V_c and V_s as indicated in equation (5)

$$V_n = V_c + V_s \tag{A.5}$$

whereV$_s$ for shear reinforcement shall be calculated by

$$\mathrm{V_s} = \frac{\mathrm{A_{sv} f_{yv}} d}{\mathrm{s}} \tag{A.6}$$

where

$\mathrm{A_{sv}}$ is the cross-section area of the shear reinforcement

$\mathrm{f_{yv}}$ is the yield strength of the shear reinforcement

s is the spacing of the stirrups

IStructE

Shear resistance that can be sustained by concrete is obtained from the momentM_c, at a distance equal to the shear span a_v, corresponding to shear failure, as follows:

$$V_c = \frac{M_c}{a_v} \tag{A7}$$

$$M_c = 0.875 a_v d \left(0.342 b_1 + 0.3 \frac{M_f}{d^2} \sqrt{\frac{z}{a_v}}\right) \sqrt[4]{\frac{16.66}{\rho_w f_y}} \tag{A8}$$

where

a_v is the shear span (mm)

d is the effective depth (mm)

b_1 is the effective width (mm) given by the lesser of $b_o + 2b_s$, $b_o + 2d_s$, with b_o, b_s, d_s, as shown in Figure A1

M_f is the flexural capacity (Nmm)

z is the lever arm (mm)

$$\rho_w = \frac{A_{sl}}{b_w d}$$

A_{sl} is the area of tensile longitudinal reinforcement (mm^2)

b_w is the web width (mm)

f_y is the characteristic strength of the tension steel (N/mm^2)

Finally, in a member with shear reinforcement, shear resistance is the sum of the shear strength of concrete, V_c,and the shear strength of the shear reinforcement as calculated by the ACI above.

List of figures

Figure 1: Shear stress distributions for (a) rectangular and (b) T sections

Figure 2: Mechanisms of load transfer through cantilever action

Figure 3: Relation between bending moment corresponding to load-carrying capacity and shear span for various percentages of longitudinal reinforcement with regions I and IV indicating ductile and II and III brittle types of failure.

Figure 4: Horizontal splitting of the compressive zone occurring at a distance of around 2.5*d* from nearest support between tip of inclined crack and extreme compressive

Figure 5:Tensile stress concentration developing in RC beams for local equilibrium purposes at location with a distance of 2.5d from the nearest support

Figure 6:Rapidly diminishing transverse tensile stresses on either side of the location of the peak value of f_t to zero at a distance of *d* and equivalent uniform stress block with intensity $0.25f_t$

Figure 7: Proposed stress blocks in web and flanges across a t-beam's width

Figure 8: Normal distribution of normalised values of load-carrying capacity of RC T-beam specimens without stirrups

Figure 9: Normal distribution of normalised values of load-carrying capacity of RC T-beam specimens with stirrups

Figure A1: Definition of b_1 for two common types of T-beam cross sections

List of Tables

Figure 1

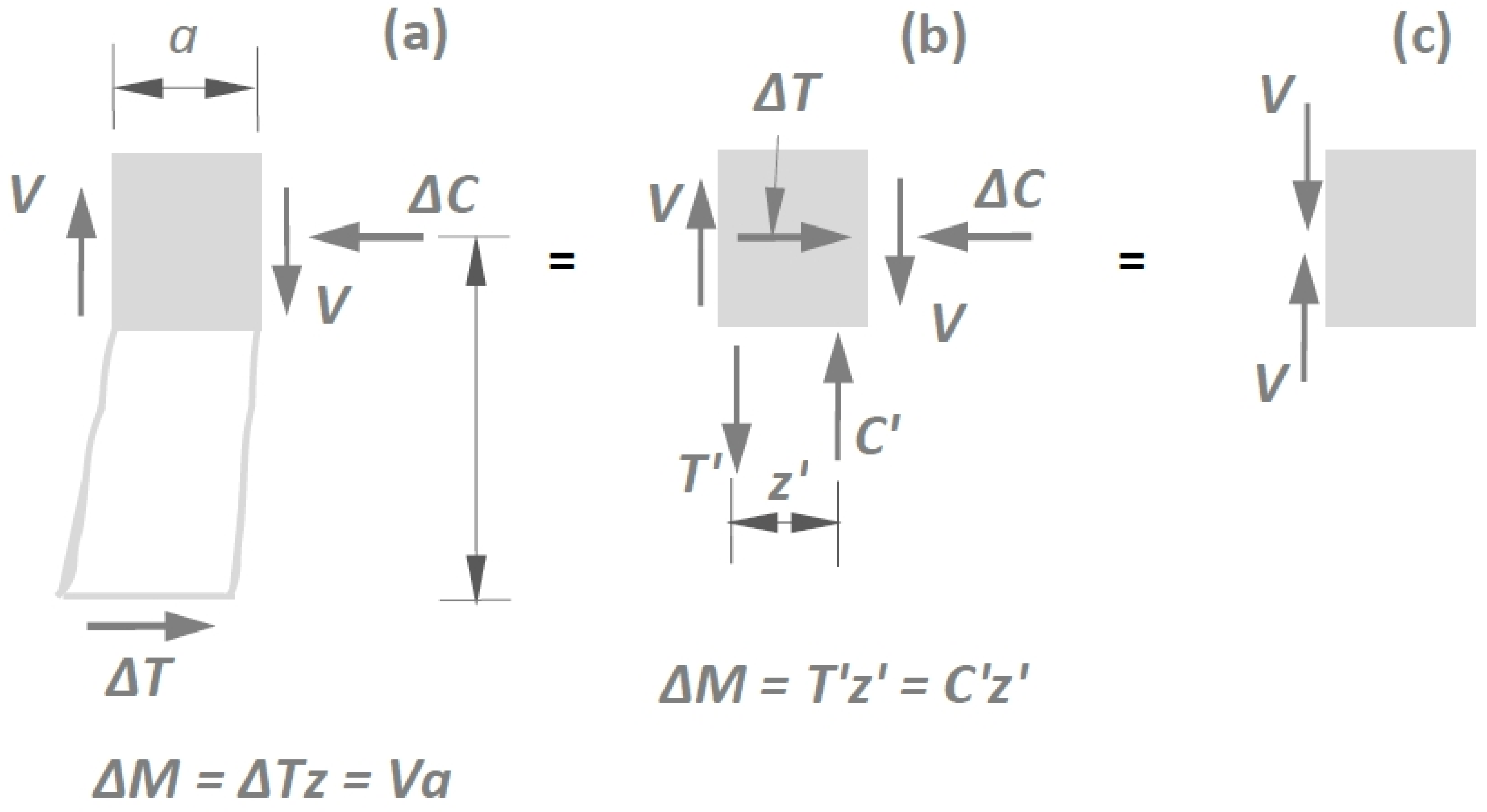

Figure 2

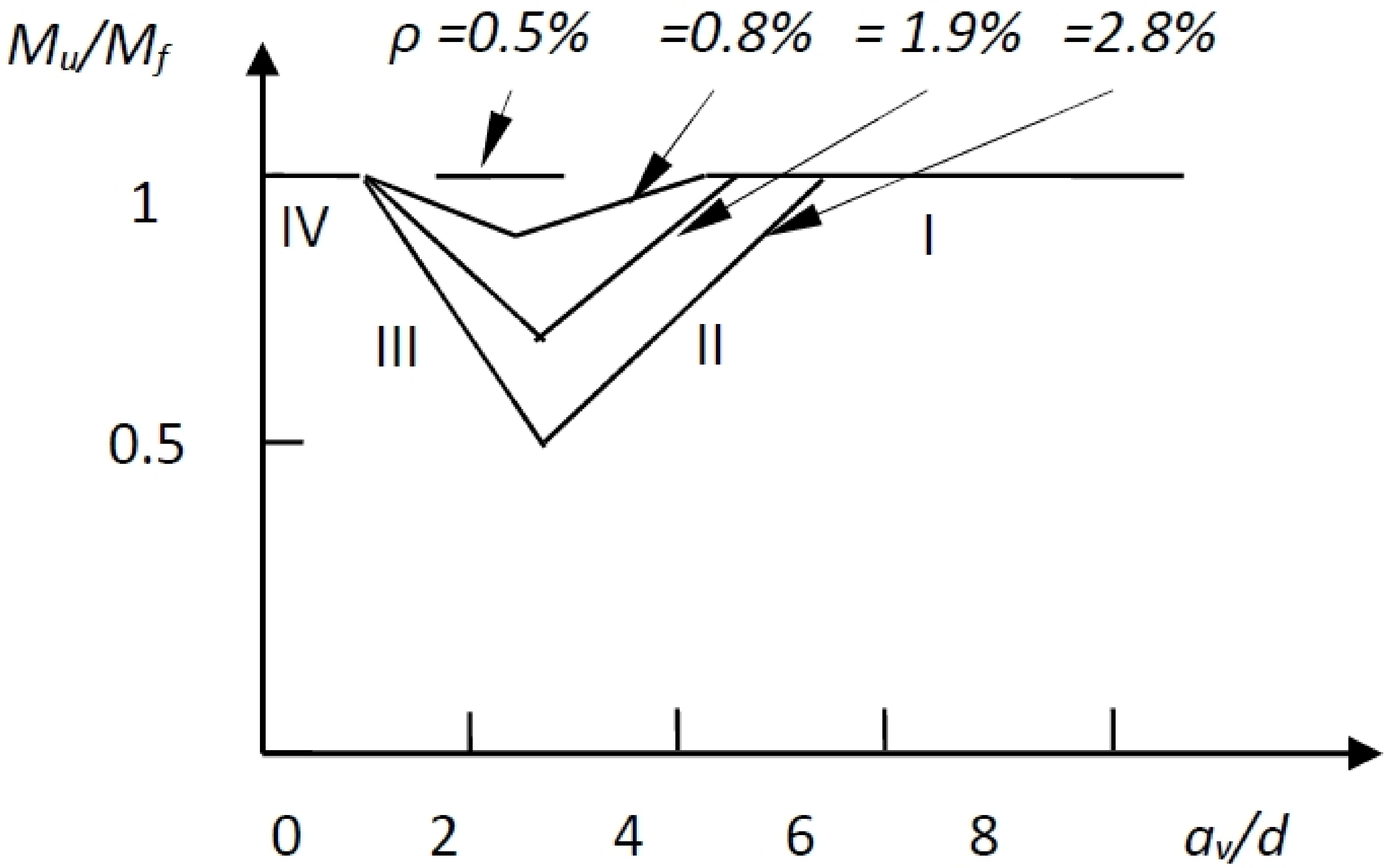

Figure 3

Figure 4

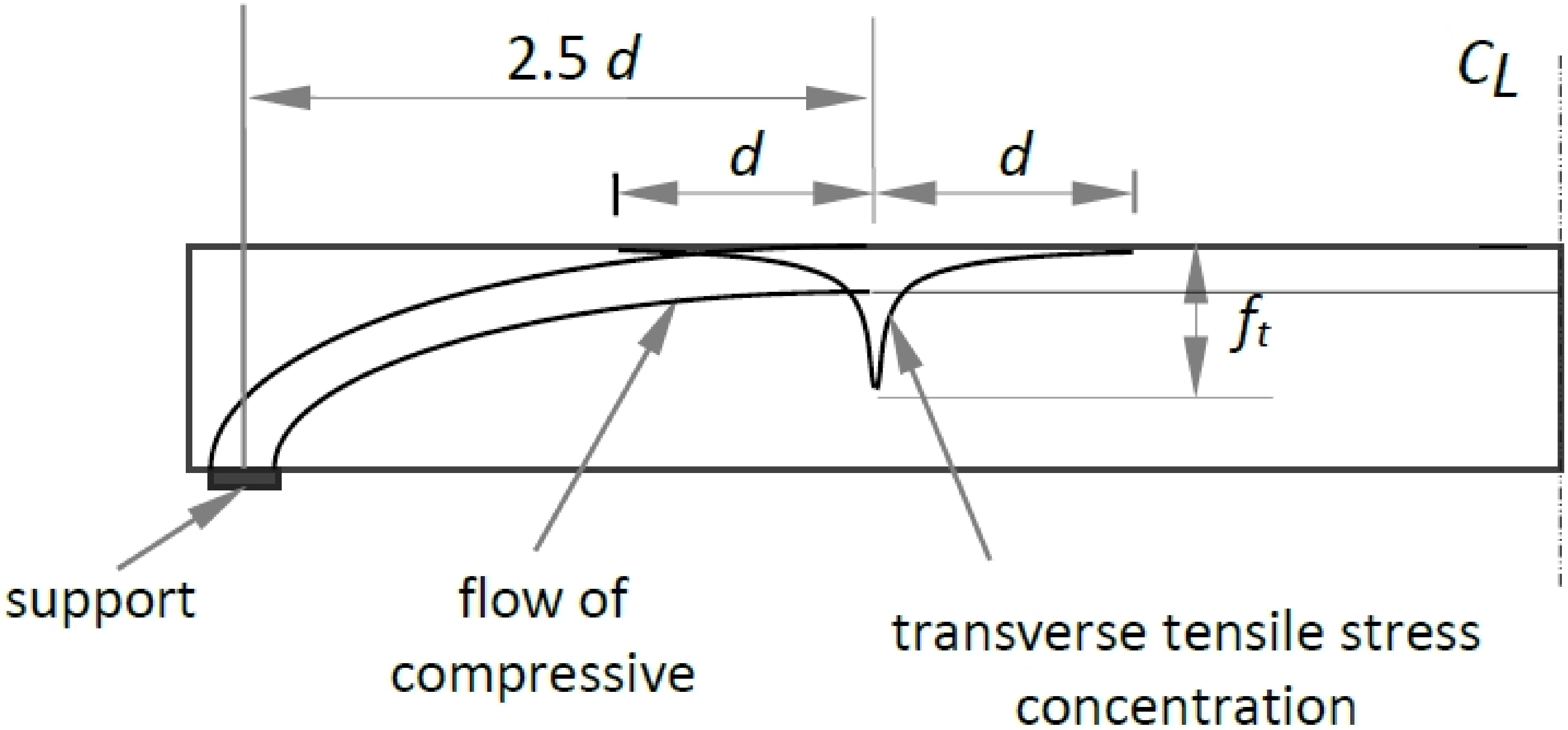
2.5 d
d
d
C_L
f_t
support
flow of
compressive
transverse tensile stress
concentration

Figure 5

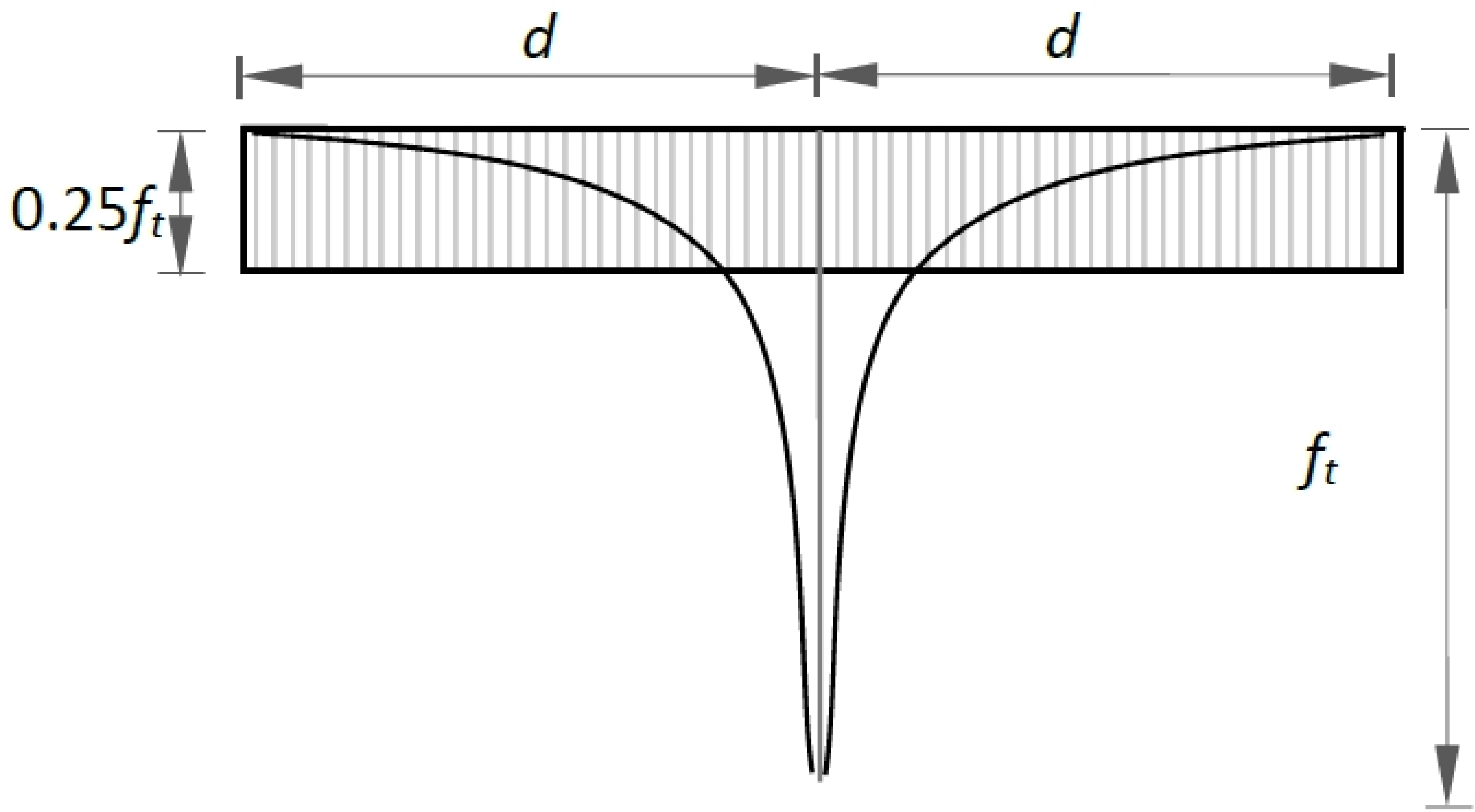

Figure 6

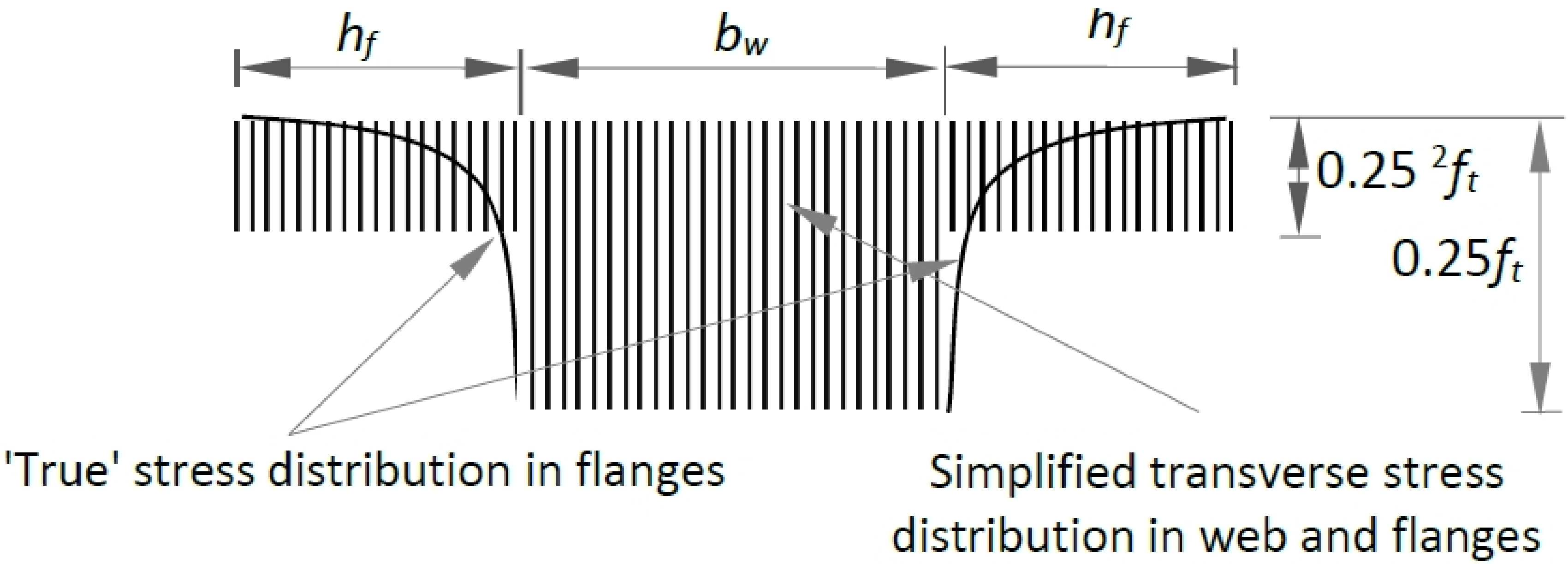

hf
bw
hf
0.25 ²ft
0.25ft
'True' stress distribution in flanges
Simplified transverse stress distribution in web and flanges

Figure 7

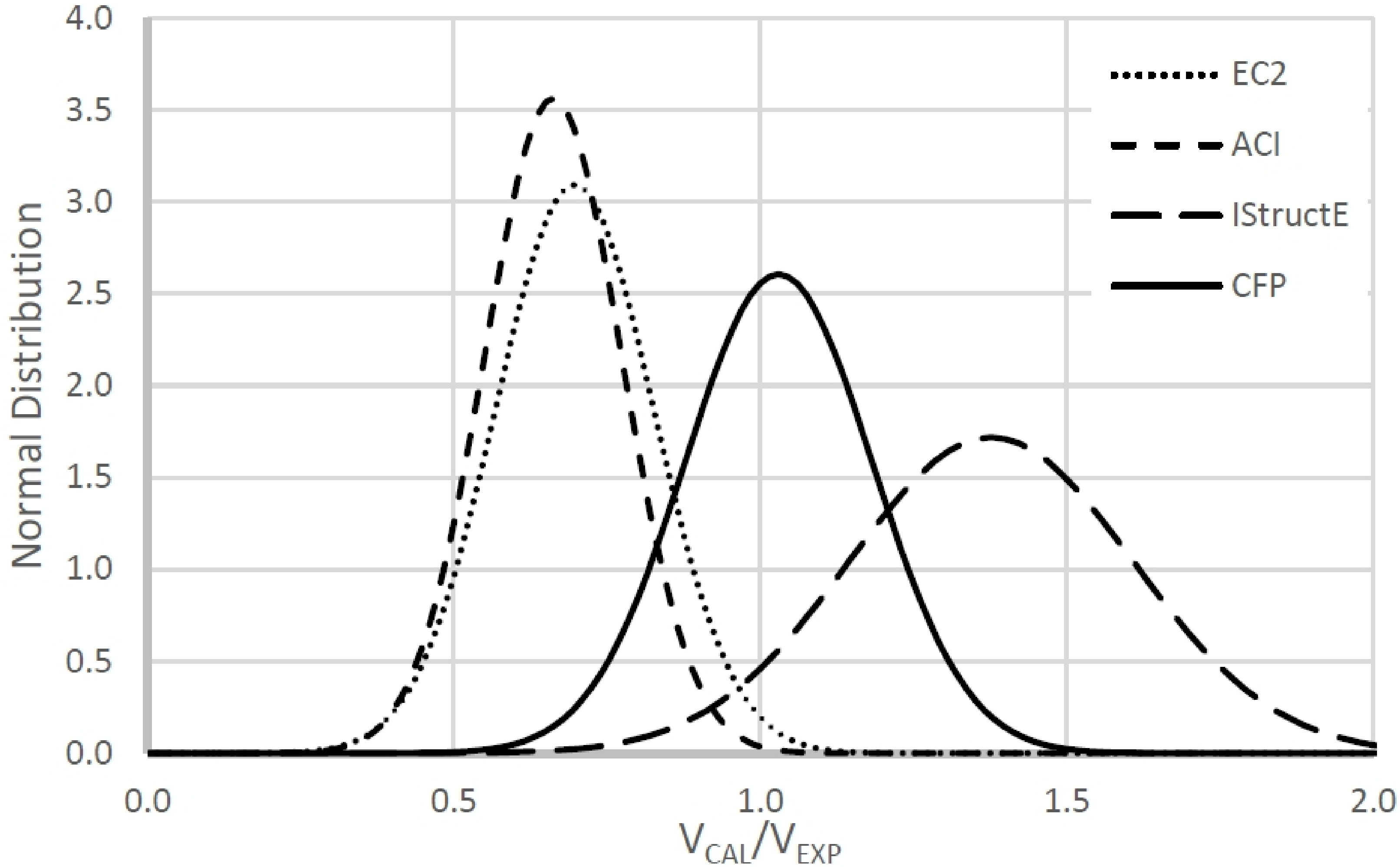

4.0
3.5
3.0
2.5
2.0
1.5
1.0
0.5
0.0
Normal Distribution
0.0
0.5
1.0
1.5
2.0
VCAL/VEXP
EC2
ACI
IStructE
CFP

Figure 8

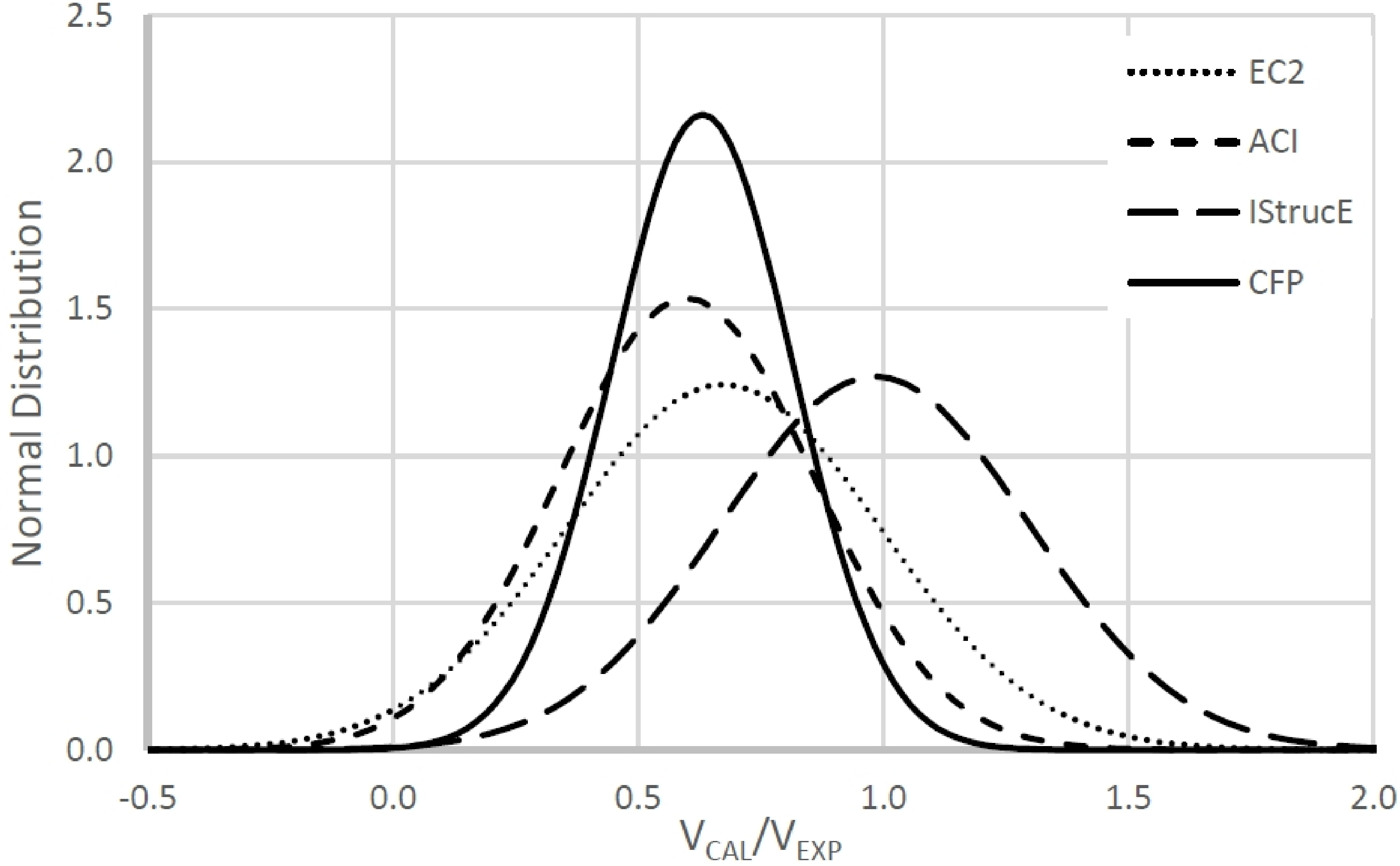

2.5
2.0
1.5
1.0
0.5
0.0
Normal Distribution
-0.5
0.0
0.5
1.0
1.5
2.0
V_CAL/V_EXP
EC2
ACI
IStrucE
CFP

Figure 9

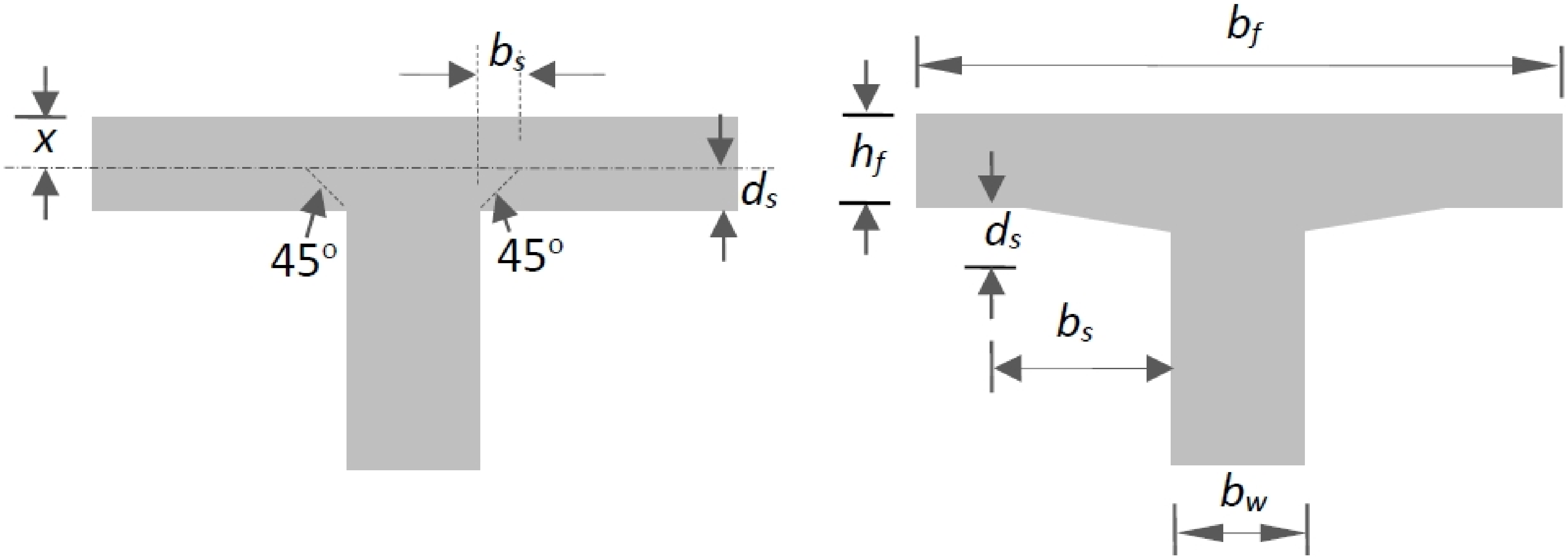

Figure A1

Table 1: Design characteristics of RC T-beam specimens without shear reinforcement

No	Specimens	Materials & Geometry										V_{EXP}
		f_c	b_w	h_f	b_f	d	ρ	f_y	ρ'	f_y'	a_v/d	
		(MPa)	(mm)	(mm)	(mm)	(mm)	(%)	(MPa)	(%)	(Mpa)	-	(kN)
Bousselham A. &Chaallal O. [9]												
1	SB-S0-0L	25.0	152	102	508	350	3.76	650	1.13	650	3.0	81.3
Ferguson P.M.& Thompson J.N. [10]												
2	A1	29.7	102	38	432	210	4.78	276	-	-	3.4	29.1
3	A2	27.3	102	38	432	210	4.78	276	-	-	3.4	27.0
4	A3	35.1	102	38	432	210	4.78	276	-	-	3.4	33.6
5	A4	34.9	102	38	432	210	4.78	276	-	-	3.4	31.6
6	A5	45.4	102	38	432	210	4.78	276	-	-	3.4	33.9
7	A6	38.7	102	38	432	210	4.78	276	-	-	3.4	35.6
8	D1	31.3	178	38	432	210	2.73	276	-	-	3.4	48.7
9	D2	29.6	178	38	432	210	2.73	276	-	-	3.4	52.1
10	N1	20.7	108	38	483	178	2.97	276	-	-	4.0	23.8
11	N2	20.6	108	38	483	178	2.97	276	-	-	4.0	23.9
12	N3	17.5	108	38	483	178	2.97	276	-	-	4.0	21.5
Kotsovos et al [11]												
13	III	40.4	50	50	200	240	5.23	540	-	-	3.3	37.0
Panda et al [12]												
14	S0-0L	46.2	100	60	250	225	2.79	500	0.89	503	3.3	50.0
Placas& Regan [13]												
15	T2	28.1	152	76	610	254	1.46	621	-	-	3.4	54.7
16	T18	28.4	152	76	610	254	4.16	621	-	-	3.6	74.7
Sahoo et al [14]												
17	TB0.00_2.5	23.2	150	50	300	217	1.85	500	0.96	500	2.5	43.5
18	TB0.00_3.0	23.2	150	50	300	217	1.85	500	0.96	500	3.0	40.0
Thamrin et al [1]												
19	T-01E	32.0	125	70	250	219	0.97	550	-	-	3.7	36.6
20	T-02E	32.0	125	70	250	219	1.45	550	-	-	3.7	38.5
21	T-03E	32.0	125	70	250	212	2.50	550	-	-	3.8	47.5
22	R-01E	32.0	125	0	0	219	0.97	550	-	-	3.7	32.6
23	R-02E	32.0	125	0	0	219	1.45	550	-	-	3.7	37.0
24	R-03E	32.0	125	0	0	212	2.50	550	-	-	3.8	37.6
Wehr K. E. [15]												
25	SS-I	27.7	152	76	914	279	1.33	1118	-	-	3.88	44.5
26	SS-II	31.4	152	76	762	279	1.33	1118	-	-	3.88	50.9
27	SS-III	29.6	152	76	610	279	1.33	1118	-	-	3.88	44.5
28	SS-IV	24.0	152	0	152	279	1.33	1118	-	-	3.88	48.7

Table 2: Design characteristics of RC T-beam specimens with shear reinforcement

No	Specimen	Materials & Geometry											Results	
		fc	b_w	h_f	b_f	*d*	*ρ*	f_y	*ρ'*	f_y	$\rho_v f_{yv}$	a_v/d	V_{EXP}	FM_{EXP}
		(MPa)	(mm)	(mm)	(mm)	(mm)	(%)	(MPa)	(%)	(MPa)		-	(kN)	
Bousselham A.&Chaallal O. [9]														
1	SB-S1_0L	25	152	102	508	350	3,76	470	1,13	470	2,456	3	263,0	S
2	SB-S2-0L	25	152	102	508	350	3,76	470	1,13	470	4,912	3	295,2	F
Koutas L. & Triantafillou T.C. [16]														
3	plain		140	80	300	263	2,76	546	2,76	523	3,938	2,3	74	S
Leonhardt F. & Walther R [17,18]														
4	ET1	22,6	300	0	300	300	1,39	430	-	-	0,570	3,5	144,5	S
5	ET2	23	150	75	300	300	2,78	430	-	-	1,160	3,5	134,5	S
6	ET3	23	100	75	300	300	4,17	430	-	-	1,730	3,5	130	S
7	ET4	23	50	75	300	300	8,34	430	-	-	3,460	3,5	101	S
8	TA3	15,4	160	80	960	375	4,40	430	-	-	2,510	3,33	283	S
9	TA4	15,4	160	80	960	375	4,40	430	-	-	1,530	3,33	239,5	S
10	TA15	17,4	160	80	960	375	4,40	430	-	-	2,510	3,33	303,5	S
11	TA11	24,9	160	80	960	375	4,40	430	-	-	2,510	3,33	347,5	S
12	TA12	24,9	160	80	960	375	4,40	430	-	-	1,530	3,33	375,5	S
13	TA16	17,4	160	80	960	375	4,40	430	-	-	2,510	3,33	304,5	S
Placas A. & Regan P.E. [13]														
14	T1	27,9	152,4	76,2	609,6	254	1,25	620,5	-	-	0,576	3,36	109,9	S
15	T3	27,5	152,4	76,2	609,6	254	1,46	620,5	-	-	0,576	3,36	104,5	S
16	T4	32,5	152,4	76,2	609,6	254	1,95	620,5	-	-	0,576	3,36	109,4	S
17	T5	33,7	152,4	76,2	609,6	254	1,46	620,5	-	-	1,151	3,36	139,7	S
18	T6	25,8	152,4	76,2	609,6	254	4,16	620,5	-	-	2,248	3,6	204,6	S
19	T7	27,4	152,4	76,2	609,6	254	3,00	620,5	-	-	0,576	3,46	109,4	S
20	T8	31,2	152,4	76,2	609,6	254	4,16	620,5	-	-	0,576	3,6	124,6	S
21	T9	20,2	152,4	76,2	609,6	254	4,16	620,5	-	-	1,151	3,6	154,4	S
22	T10	28,2	152,4	76,2	609,6	254	1,46	620,5	-	-	0,384	3,36	86,7	S
23	T11	37	152,4	76,2	609,6	254	4,16	620,5	-	-	1,151	3,6	160,1	S
24	T12	30,7	152,4	76,2	609,6	254	4,16	620,5	-	-	0,576	3,6	144,6	S
25	T13	33,4	152,4	76,2	609,6	254	1,46	620,5	-	-	0,576	3,36	89,9	S
26	T14	33,4	152,4	76,2	609,6	254	4,16	620,5	-	-	2,248	3,6	219,3	S
27	T15	33,2	152,4	76,2	609,6	254	4,16	620,5	-	-	0,576	7,2	104,5	S
28	T16	32,7	152,4	76,2	609,6	254	4,16	620,5	-	-	0,384	7,2	92,5	S
29	T17	33	152,4	76,2	609,6	254	4,16	620,5	-	-	1,151	7,2	133,9	S
30	T19	29,9	152,4	76,2	609,6	254	4,16	620,5	-	-	0,576	5,4	113,4	S
31	T20	32,1	152,4	76,2	609,6	254	4,16	620,5	-	-	1,151	5,4	153,9	S
32	T22	34,3	152,4	76,2	609,6	254	1,46	620,5	-	-	0,576	3,36	109,4	S
33	T25	54,1	152,4	76,2	609,6	254	1,46	620,5	-	-	0,576	3,36	114,8	S
34	T26	57	152,4	76,2	609,6	254	4,16	620,5	-	-	1,151	3,6	179,3	S
35	T27	12	152,4	76,2	609,6	254	4,16	620,5	-	-	1,151	3,6	132,1	S
36	T31	31	152,4	76,2	609,6	254	1,46	620,5	-	-	0,576	3,36	94,7	S
37	T32	27,6	152,4	76,2	609,6	254	4,16	620,5	-	-	2,248	3,6	216,2	S
38	T33	36,8	152,4	76,2	609,6	254	1,46	620,5	-	-	1,151	4,5	109,4	F
39	T34	33,9	152,4	76,2	609,6	254	4,16	620,5	-	-	0,576	5,4	112,1	S
40	T35	33,6	152,4	76,2	609,6	254	4,16	620,5	-	-	0,576	5,4	114,8	S
41	T36	24,1	152,4	76,2	609,6	254	4,16	620,5	-	-	1,151	3,6	179,3	S
42	T37	31,8	152,4	76,2	609,6	254	4,16	620,5	-	-	2,248	3,6	209,5	S
43	T38	30,2	152,4	76,2	609,6	254	4,16	620,5	-	-	2,248	3,6	239,3	S
Sorensen H.C. [19]														
44	T21	32,5	110	80	400	298	3,83	420	-	-	1,301	3,5	129	S
45	T22	31,1	110	80	400	298	3,83	420	-	-	1,307	3,5	127	S
46	T23	34,2	110	80	400	298	3,83	420	-	-	1,187	3,5	139	S
47	T1a	22,9	110	80	400	298	3,83	457	0,61	262	1,523	3,5	132	F
48	T2a	24,6	110	80	400	298	3,83	457	0,61	262	1,592	3,5	136	F
49	T3a	24,6	110	80	400	298	3,83	457	0,61	262	1,269	3,5	127	S
50	T4a	25,2	110	80	400	298	3,83	457	0,61	262	1,327	3,5	132	S
51	T1b	23,1	110	80	400	298	3,83	457	0,61	262	1,139	3,5	118	S
52	T2b	24,9	110	80	400	298	3,83	457	0,61	262	1,191	3,5	129	S
53	T3b	24,6	110	80	400	298	3,83	457	0,61	262	0,762	3,5	116	S
54	T4b	24,7	110	80	400	298	3,83	457	0,61	262	0,796	3,5	107	S
55	T5	25,5	110	80	400	298	3,83	457	0,61	262	0,796	3,5	110	S
Spangolo et al [20]														
56	VR1	48,44	150	80	400	360	2,23	600	0,07	596	1,562	2,4	203,61	S
57	VR2	49,92	150	80	400	360	2,23	600	0,07	596	0,781	2,4	151,25	S

Table 3: Calculated values of shear load corresponding to flexural (V_f) and shear (V_c) types of failure and experimentally-established values of shear at failure and modes of failure of T-Beams without transverse reinforcement

No	Specimen	Experimental Results		Calculated values of shear load at failure and mode of failure											
				EC2[3]			ACI318 [2]			IStructE[5]			Proposed		
		V_{EXP}	FM_{EXP}	V_f	V_c	FM	V_f	V_c	FM	V_f	V_s	FM	V_f	V_c	FM
		(kN)	-	(kN)	(kN)	-	(kN)	(kN)	-	(kN)	(kN)	-	(kN)	(kN)	-
1	SB-S0-0L	81.3	S	164.4	51.0	S	192.3	45.2	S	164.4	159.3	S	389.1	70.8	S
2	A1	29.1	S	78.5	26.4	S	77.7	19.7	S	78.5	47.3	S	79.7	29.7	S
3	A2	27.0	S	78.1	25.6	S	77.3	18.9	S	78.1	46.7	S	79.4	27.4	S
4	A3	33.6	S	79.1	27.9	S	78.5	21.4	S	79.1	48.4	S	80.2	34.4	S
5	A4	31.6	S	79.1	27.8	S	78.5	21.4	S	79.1	48.4	S	80.2	34.2	S
6	A5	33.9	S	80.0	30.4	S	79.5	24.4	S	80.0	49.7	S	80.7	42.7	S
7	A6	35.6	S	79.5	28.8	S	78.9	22.5	S	79.5	48.9	S	80.4	37.4	S
8	D1	48.7	S	78.7	38.9	S	78.0	35.4	S	78.7	60.7	S	79.9	50.8	S
9	D2	52.1	S	78.5	38.2	S	77.7	34.5	S	78.5	60.2	S	79.7	48.3	S
10	N1	23.8	S	37.6	18.2	S	37.3	14.9	S	37.6	32.2	S	38.2	23.4	S
11	N2	23.9	S	37.6	18.2	S	37.3	14.8	S	37.6	32.2	S	38.2	23.3	S
12	N3	21.5	S	37.3	17.2	S	36.9	13.7	S	37.3	31.5	S	38	19.8	S
13	III	37.0	S	92.8	16.4	S	91.3	13.0	S	92.8	40.1	S	95.2	32.8	S
14	S0-0L	50.0	S	90.6	26.5	S	76.1	26.0	S	90.6	54.1	S	93.3	41.0	S
15	T2	54.7	S	100.1	30.2	S	99.4	34.9	S	100.1	77.4	S	101.3	53.9	S
16	T18	74.7	S	246.0	43.0	S	212.4	35.1	S	246.0	114.3	S	254.9	54.5	S
17	TB0.00_2.5	43.5	S	112	26.8	S	111.4	26.7	S	112	64.3	S	114.3	46.3	S
18	TB0.00_3.0	40.0	S	93.6	26.8	S	93.1	26.7	S	93.6	59.9	S	95.5	44.1	S
19	T-01E	36.6	S	38.3	20.2	S	38.0	26.3	S	38.3	44.1	F	38.8	41.1	S
20	T-02E	38.5	S	56.2	23.1	S	55.5	26.3	S	56.2	48.3	S	57.3	44.0	S
21	T-03E	47.5	S	86.3	27.0	S	84.5	25.5	S	86.3	53.6	S	89.3	42.6	S
22	R-01E	32.6	S	36.6	20.2	S	36.1	26.3	S	36.6	34.3	S	37.6	34.3	S
23	R-02E	37.0	S	52.5	23.1	S	51.1	26.3	S	52.5	39.4	S	54.6	34.3	S
24	R-03E	37.6	S	75.9	27.0	S	72.7	25.5	S	75.9	44.3	S	81.8	33.3	S
25	SS-I	44.5	S	70.7	31.4	S	70.4	38.1	S	70.7	74.9	F	71.1	58.6	S
26	SS-II	50.9	S	70.6	32.8	S	70.3	40.6	S	70.6	74.7	F	71	65.7	S
27	SS-III	44.5	S	70.1	32.1	S	69.7	39.4	S	70.1	73.1	F	70.7	62.2	S
28	SS-IV	48.7	S	62	30.0	S	60.2	35.5	S	62	53.7	S	65.4	51.1	S

Table 4: Calculated and experimentally-established values of shear load of RC T-beams without web reinforcement exhibiting a shear mode of failure

No	Specimen	V_{EXP}	V_{EC2}	V_{EC2}/V_{EXP}	V_{ACI}	V_{ACI}/V_{EXP}	$V_{IStructE}$	$V_{IStructE}$ $/V_{EXP}$	$V_{proposed}$	$V_{proposed}$ $/V_{EXP}$
		(kN)	**(kN)**	-	**(kN)**	-	**(kN)**	-	**(kN)**	-
1	SB-S0-0L	81.3	51.0	0.628	45.2	0.556	159.3	1.960	70.8	0.871
2	A1	29.1	26.4	0.907	19.7	0.677	47.3	1.627	29.7	1.021
3	A2	27.0	25.6	0.948	18.9	0.700	46.7	1.731	27.4	1.015
4	A3	33.6	27.9	0.830	21.4	0.637	48.4	1.440	34.4	1.024
5	A4	31.6	27.8	0.880	21.4	0.677	48.4	1.531	34.2	1.082
6	A5	33.9	30.4	0.897	24.4	0.720	49.7	1.467	42.7	1.260
7	A6	35.6	28.8	0.809	22.5	0.632	48.9	1.375	37.4	1.051
8	D1	48.7	38.9	0.799	35.4	0.727	60.7	1.246	50.8	1.043
9	D2	52.1	38.2	0.733	34.5	0.662	60.2	1.156	48.3	0.927
10	N1	23.8	18.2	0.765	14.9	0.626	32.2	1.355	23.4	0.983
11	N2	23.9	18.2	0.762	14.8	0.619	32.2	1.348	23.3	0.975
12	N3	21.5	17.2	0.800	13.7	0.637	31.5	1.465	19.8	0.921
15	III	37.0	16.4	0.443	13.0	0.351	40.1	1.083	32.8	0.886
16	S0-0L	50.0	26.5	0.530	26.0	0.520	54.1	1.082	41.0	0.820
17	T2	54.7	30.2	0.552	34.9	0.638	77.4	1.415	53.9	0.985
18	T18	74.7	43.0	0.576	35.1	0.470	114.3	1.530	54.5	0.730
19	TB0.00_2.5	43.5	26.8	0.616	26.7	0.614	64.3	1.479	46.3	1.064
20	TB0.00_3.0	40.0	26.8	0.670	26.7	0.668	59.9	1.498	44.1	1.103
21	T-01E	36.6	20.2	0.552	26.3	0.719	44.1	1.206	41.1	1.123
22	T-02E	38.5	23.1	0.600	26.3	0.683	48.3	1.254	44.0	1.143
23	T-03E	47.5	27.0	0.568	25.5	0.537	53.6	1.129	42.6	0.897
24	R-01E	32.6	20.2	0.620	26.3	0.807	34.3	1.052	34.3	1.052
25	R-02E	37.0	23.1	0.624	26.3	0.711	39.4	1.065	34.3	0.927
26	R-03E	37.6	27.0	0.718	25.5	0.678	44.3	1.178	33.3	0.886
27	SS-I	44.5	31.4	0.706	38.1	0.857	74.9	1.684	58.6	1.317
28	SS-II	50.9	32.8	0.644	40.6	0.797	74.7	1.466	65.7	1.291
29	SS-III	44.5	32.1	0.722	39.4	0.886	73.1	1.644	62.2	1.399
30	SS-IV	48.7	30.0	0.616	35.5	0.729	53.7	1.103	51.1	1.050
	AVR			**0.697**		**0.662**		**1.377**		**1.030**
	STD			**0.129**		**0.112**		**0.232**		**0.153**

Table 5: Calculated values of shear load corresponding to flexural and shear modes of failure and experimentally-established values of shear load at failure and modes of failure of T-Beams with web reinforcement

No	Name specimens	Experimental results		Calculated value of shear load at failure (kN) and mode of failure											
				EC2 [3]			ACI 318 [2]			IStructE[5]			proposed		
		V_{EXP}	FM	V_f	V_c	FM	V_f	V_c	FM	V_f	V_c	FM	V_f	V_c	FM
1	SB-S1_0L	263,0	S	289.9	254.7	S	298.5	175.9	S	289.9	278.5	S	294.1	217.9(s)	S
2	SB-S2-0L	295,2	F	289.9	319.5	F	298.5	298.5	F	289.9	409.1	F	294.1	217.9(s)	S
3	plain	74,0	S	216.6	194.8	S	230.3	174.7	S	216.6	244.2	F	223.3	71.3(s)	S
4	ET1	144,5	S	133.4	115.4	S	129.8	124.0	S	133.4	141.9	F	140.1	102.6(s)	S
5	ET2	134,5	S	67.7	117.5	F	129.4	88.9	S	67.7	95.3	F	140.4	104.4(s)	S
6	ET3	130,0	S	88.3	116.8	F	128.6	76.4	S	88.3	94.9	F	140.4	103.8(s)	S
7	ET4	101,0	S	108.9	77.4	S	126.3	64.1	S	108.9	90.1	S	140.4	103.8(s)	S
8	TA3	283,0	S	304.5	217.4	S	297.2	190.6	S	304.5	304.4	S	317.6	301.2(s)	S
9	TA4	239,5	S	304.5	182.1	S	297.2	131.8	S	304.5	245.6	S	317.6	183.6(s)	S
10	TA15	303,5	S	304.5	234.9	S	304.5	193.1	S	304.5	323.9	F	320.3	301.2(s)	S
11	TA11	347,5	S	319.3	289.1	S	315.5	201.5	S	319.3	315.9	S	326.5	301.2(s)	S
12	TA12	375,5	S	319.3	206.6	S	315.5	142.7	S	319.3	257.1	S	326.5	183.6(s)	S
13	TA16	304,5	S	304.5	234.9	S	304.5	193.1	S	304.5	303.1	S	320.3	301.2(s)	S
14	T1	109,9	S	86.3	50.1	S	85.7	57.0	S	86.3	95.6	F	87.1	44.6(c)	S
15	T3	104,5	S	100.1	50.1	S	99.3	56.8	S	100.1	99.5	S	101.3	44.6(c)	S
16	T4	109,4	S	132.9	50.1	S	131.8	59.8	S	132.9	110.2	S	134.7	49.2(c)	S
17	T5	139,7	S	100.9	100.3	S	100.2	82.8	S	100.9	123.3	F	101.8	89.1(s)	S
18	T6	204,6	S	242.7	181.9	S	235.9	120.4	S	242.7	196.1	S	252.7	174.0(s)	S
19	T7	109,4	S	190.6	50.1	S	187.5	56.7	S	190.6	123.4	S	195.6	44.6(c)	S
20	T8	124,6	S	248.9	50.1	S	243.8	59.0	S	248.9	139.3	S	257.0	47.5(c)	S
21	T9	154,4	S	169.5	100.3	S	219.0	74.1	S	169.5	117.1	S	248.0	89.1(s)	S
22	T10	86,7	S	100.2	33.4	S	99.4	49.8	S	100.2	92.3	S	101.4	43.3(c)	S
23	T11	160,1	S	253.4	100.3	S	249.1	84.6	S	253.4	165.8	S	260.1	89.1(s)	S
24	T12	144,6	S	248.4	50.1	S	243.2	58.7	S	248.4	138.9	S	256.6	46.8(c)	S
25	T13	89,9	S	100.8	50.1	S	100.2	60.3	S	100.8	101.0	F	101.8	50.4(c)	S
26	T14	219,3	S	250.7	195.8	S	246.0	125.0	S	250.7	205.8	S	258.3	174.0(s)	S
27	T15	104,5	S	125.3	50.1	S	122.9	60.2	S	125.3	109.8	S	129.1	50.2(c)	S
28	T16	92,5	S	125.1	33.4	S	122.7	52.5	S	125.1	102.1	S	128.9	49.5(c)	S
29	T17	133,9	S	125.2	100.3	S	122.8	82.4	S	125.2	132.0	F	129.0	89.1(s)	S
30	T19	113,4	S	165.1	50.1	S	120.1	58.3	S	165.1	119.0	S	170.7	45.7(c)	S
31	T20	153,9	S	166.4	100.3	S	163.2	81.9	S	166.4	142.9	S	171.7	89.1(s)	S
32	T22	109,4	S	100.9	50.1	S	100.3	60.8	S	100.9	101.2	F	101.9	51.6(c)	S
33	T25	114,8	S	102.1	50.1	S	101.8	70.7	S	102.1	103.4	F	102.8	75.1(c)	S
34	T26	179,3	S	261.3	100.3	S	259.1	94.3	S	261.3	173.3	S	266.0	89.1(c)	S
35	T27	132,1	S	103.7	91.1	S	116.9	67.4	S	103.7	39.6	S	227.8	89.1(s)	S
36	T31	94,7	S	100.6	50.1	S	99.9	58.9	S	100.6	100.5	S	101.6	47.2(c)	S
37	T32	216,2	S	245.1	188.4	S	235.9	121.6	S	245.1	200.5	S	254.3	174.0	S
38	T33	109,4	F	75.5	100.3	F	75.1	84.5	F	75.5	116.3	F	76.2	89.1(s)	F
39	T34	112,1	S	167.4	50.1	S	164.3	60.6	S	167.4	121.9	S	172.4	51.1(c)	S
40	T35	114,8	S	167.3	50.1	S	164.1	60.4	S	167.3	121.7	S	172.3	50.7(c)	S
41	T36	179,3	S	235.9	100.3	S	233.5	76.9	S	235.9	158.7	S	252.8	89.1(s)	S
42	T37	209,5	S	249.4	195.8	S	244.4	124.1	S	249.4	204.5	S	257.3	174.0(s)	S
43	T38	239,3	S	247.9	195.8	S	181.5	123.2	S	247.9	203.1	S	256.3	174.0(s)	S
44	T21	129,0	S	139.5	96.0	S	137.7	74.4	S	139.5	124.8	S	142.4	85.3(s)	S
45	T22	127,0	S	139.1	96.4	S	137.2	73.9	S	139.1	124.2	S	142.1	85.7(s)	S
46	T23	139,0	S	140.0	87.5	S	138.3	71.5	S	140.0	121.8	S	142.7	77.8(s)	S
47	T1a	132,0	F	147.3	112.3	S	147.5	76.6	S	147.2	129.8	S	151.8	99.9(s)	S
48	T2a	136,0	F	148.1	119.6	S	148.3	79.8	S	148.1	133.4	S	152.4	104.4(s)	S
49	T3a	127,0	S	148.1	93.6	S	148.3	69.2	S	148.1	122.8	S	152.4	83.2(s)	S
50	T4a	132,0	S	148.4	99.6	S	148.6	71.5	S	148.4	125.1	S	152.0	87.0(s)	S
51	T1b	118,0	S	147.4	84.0	S	147.6	64.1	S	147.4	117.4	S	151.9	74.7(s)	S
52	T2b	129,0	S	148.2	89.4	S	148.5	66.8	S	148.2	120.5	S	152.5	78.1(s)	S
53	T3b	116,0	S	148.1	56.2	S	148.3	52.6	S	148.1	106.2	S	152.4	49.9(s)	S
54	T4b	107,0	S	148.2	59.8	S	148.4	53.8	S	148.2	107.4	S	152.5	52.2(s)	S
55	T5	110,0	S	148.5	59.8	S	148.7	54.2	S	148.5	107.9	S	152.1	52.2(s)	S
56	VR1	203,6	S	282.6	189.7	S	281.0	148.2	S	282.6	228.2	S	286.5	107.4(s)	S
57	VR2	151,3	S	283.0	94.9	S	281.5	107.0	S	283.0	186.6	S	286.8	109.7(s)	S

Table 6: Calculated and experimentally-established values of shear load of RC T-beams with web reinforcement exhibiting a shear mode of failure

No	Specimens	V_{EXP}	V_{EC2}	V_{EC2}/V_{EXP}	V_{ACI}	V_{ACI}/V_{EXP}	V_{B}	V_{B}/V_{EXP}	V_{CFP}	V_{CFP}/V_{EXP}
		(kN)	**(kN)**	-	**(kN)**	-	**(kN)**	-	**(kN)**	-
1	SB-S1_0L	263.0	254.7	0.969	175.9	0.669	278.5	1.059	217.9	0.828
2	plain	74.0	194.8	2.633	174.7	2.361	216.6	2.928	71.3	0.964
3	ET1	144.5	115.4	0.799	124.0	0.858	133.4	0.923	102.6	0.710
4	ET2	134.5	67.7	0.503	88.9	0.661	67.7	0.503	104.4	0.776
5	ET3	130.0	88.3	0.679	76.4	0.587	88.3	0.679	103.8	0.798
6	ET4	101.0	77.4	0.767	64.1	0.635	90.1	0.893	103.8	1.028
7	TA3	283.0	217.4	0.768	190.6	0.674	303.1	1.071	301.2	1.064
8	TA4	239.5	182.1	0.761	131.8	0.550	244.3	1.020	183.6	0.767
9	TA15	303.5	234.9	0.774	193.1	0.636	303.1	0.999	301.2	0.992
10	TA11	347.5	289.1	0.832	201.5	0.580	315.9	0.909	301.2	0.867
11	TA12	375.5	206.6	0.550	142.7	0.380	257.1	0.685	183.6	0.489
12	TA16	304.5	234.9	0.771	193.1	0.634	303.1	0.996	301.2	0.989
13	T1	109.9	50.1	0.456	57.0	0.519	86.3	0.785	44.6	0.406
14	T3	104.5	50.1	0.480	56.8	0.543	99.5	0.953	44.6	0.427
15	T4	109.4	50.1	0.458	59.8	0.547	110.2	1.007	49.2	0.450
16	T5	139.7	100.3	0.718	82.8	0.592	100.9	0.722	89.1	0.638
17	T6	204.6	181.9	0.889	120.4	0.589	196.1	0.958	174.0	0.851
18	T7	109.4	50.1	0.458	56.7	0.519	123.4	1.128	44.6	0.407
19	T8	124.6	50.1	0.402	59.0	0.474	139.3	1.118	47.5	0.381
20	T9	154.4	100.3	0.650	74.1	0.480	117.1	0.759	89.1	0.577
21	T10	86.7	33.4	0.386	49.8	0.575	92.3	1.065	43.3	0.499
22	T11	160.1	100.3	0.626	84.6	0.528	165.8	1.036	89.1	0.557
23	T12	144.6	50.1	0.347	58.7	0.406	138.9	0.960	46.8	0.324
24	T13	89.9	50.1	0.558	60.3	0.671	100.8	1.122	50.4	0.561
25	T14	219.3	195.8	0.893	125.0	0.570	205.8	0.938	174.0	0.794
26	T15	104.5	50.1	0.480	60.2	0.576	109.8	1.051	50.2	0.480
27	T16	92.5	33.4	0.362	52.5	0.568	102.1	1.103	49.5	0.535
28	T17	133.9	100.3	0.749	82.4	0.615	125.2	0.935	89.1	0.666
29	T19	113.4	50.1	0.442	58.3	0.514	119.0	1.049	45.7	0.403
30	T20	153.9	100.3	0.652	81.9	0.532	142.9	0.929	89.1	0.579
31	T22	109.4	50.1	0.458	60.8	0.556	100.9	0.923	51.6	0.472
32	T25	114.8	50.1	0.437	70.7	0.616	102.1	0.890	75.1	0.654
33	T26	179.3	100.3	0.559	94.3	0.526	173.3	0.967	89.1	0.497
34	T27	132.1	91.1	0.689	67.4	0.510	39.6	0.299	89.1	0.675
35	T31	94.7	50.1	0.529	58.9	0.622	100.5	1.061	47.2	0.499
36	T32	216.2	188.4	0.872	121.6	0.562	200.5	0.927	174.0	0.805
37	T34	112.1	50.1	0.447	60.6	0.541	121.9	1.087	51.1	0.456
38	T35	114.8	50.1	0.437	60.4	0.526	121.7	1.060	50.7	0.442
39	T36	179.3	100.3	0.559	76.9	0.429	158.7	0.885	89.1	0.497
40	T37	209.5	195.8	0.934	124.1	0.592	204.5	0.976	174.0	0.831
41	T38	239.3	195.8	0.818	123.2	0.515	203.1	0.849	174.0	0.727
42	T21	129.0	96.0	0.744	74.4	0.577	124.8	0.967	85.3	0.661
43	T22	127.0	96.4	0.759	73.9	0.582	124.2	0.978	85.7	0.675
44	T23	139.0	87.5	0.630	71.5	0.514	121.8	0.876	77.8	0.560
45	T3a	127.0	93.6	0.737	69.2	0.545	122.8	0.967	83.2	0.655
46	T4a	132.0	99.6	0.755	71.5	0.541	125.1	0.948	87.0	0.659
47	T1b	118.0	84.0	0.712	64.1	0.543	117.4	0.995	74.7	0.633
48	T2b	129.0	89.4	0.693	66.8	0.518	120.5	0.934	78.1	0.605
49	T3b	116.0	56.2	0.484	52.6	0.453	106.2	0.915	49.9	0.430
50	T4b	107.0	59.8	0.559	53.8	0.503	107.4	1.003	52.2	0.488
51	T5	110.0	59.8	0.543	54.2	0.493	107.9	0.981	52.2	0.474
52	VR1	203.6	189.7	0.932	148.2	0.728	228.2	1.121	107.4	0.527
53	VR2	151.3	94.9	0.627	107.0	0.708	186.6	1.234	109.7	0.725
	AVR			**0.674**		**0.599**		**0.983**		**0.631**
	STV			**0.321**		**0.260**		**0.314**		**0.185**